Sub-shot-noise photon-number correlation in a mesoscopic twin beam of light

Maria Bondani,[1,*] Alessia Allevi,[2] Guido Zambra,[3,4] Matteo G. A. Paris,[4] and Alessandra Andreoni[2]
[1]*National Laboratory for Ultrafast and Ultraintense Optical Science, C.N.R.-I.N.F.M., Como, Italy*
[2]*C.N.R.-I.N.F.M.-C.N.I.S.M., Dipartimento di Fisica e Matematica, Università dell'Insubria, Como, Italy*
[3]*Dipartimento di Fisica e Matematica, Università dell'Insubria, Como, Italy*
[4]*Dipartimento di Fisica dell'Università di Milano, Milan, Italy*
(Received 22 December 2006; published 27 July 2007)

We demonstrate sub-shot-noise photon-number correlations in a (temporal) multimode mesoscopic ($\sim 10^3$ detected photons) twin beam produced by picosecond-pulsed spontaneous nondegenerate parametric down-conversion. We have separately detected the signal and idler distributions of photons collected in twin coherence areas and found that the variance of the photon-count difference goes below the shot-noise limit by 3.25 dB. The number of temporal modes contained in the twin beam, as well as the size of the twin coherence areas, depends on the pump intensity. Our scheme is based on spontaneous down-conversion and thus does not suffer from limitations due to the finite gain of the parametric process. Twin beams are also used to demonstrate the conditional preparation of a nonclassical (sub-Poissonian) state.

DOI: 10.1103/PhysRevA.76.013833 PACS number(s): 42.50.Dv, 42.50.Ar, 42.65.Lm

I. INTRODUCTION

Quantum correlations have been the subject of intensive investigations, and sub-shot-noise in photon-number correlations has been indeed observed through the generation of the so-called *twin beam* of light. So far twin beams have been obtained in the macroscopic regime from parametric oscillators [1–3] or from seeded parametric amplifiers [4,5] and, with much lower photon numbers, from traveling-wave optical parametric amplifiers (OPAs) [6,7]. Quantum correlations between light beams play a crucial role in fundamental quantum optics [8] and find applications in quantum cryptography [9] and communication [10,11], spectroscopy [1], and interferometry [12], as well as in enhancing sensitivity in imaging [13] and high-precision measurements [14].

Ideal twin-beam states, as those generated by traveling-wave OPAs starting from vacuum, exhibit perfect quantum correlations in the photon number for any average photon number, whereas approximations to them can be obtained by optical parametric oscillators (OPOs), where the increased intensity is obtained at the price of introducing additional noise. On the other hand, the existence of quantum correlations in mesoscopic and macroscopic twin-beam states may be demonstrated for continuous-wave OPOs via indirect measurements of the difference photocurrent by analysis in a narrow frequency bandwidth. These procedures directly give the amount of noise reduction in the system but lose information on the number of photons in each party of the twin beam. Notice that OPO-based systems are unavoidably spatially multimode [15], and show a Poissonian distribution of the intensities of signal and idler.

The shot-noise limit (SNL) in any photodetection process is defined as the lowest level of noise that can be obtained by using semiclassical states of light—that is, Glauber coherent states. If one measures the photon numbers of two beams and evaluates their difference, the SNL is the lower limit of noise that can be reached when the beams are classically correlated. On the other hand, when intensity correlations below the SNL are observed, we have a genuine quantum effect.

In this paper we present the demonstration of sub-shot-noise correlations in a twin beam obtained from a pulsed OPA starting from the vacuum state. Our scheme involves a traveling-wave OPA operating at two different frequencies. The resulting twin beams are mesoscopic (more than $\sim 10^3$ detected photons) and sub-shot-noise correlations have been demonstrated by direct measurement of the number of photons in the two parties of the twin state. This procedure yields complete information on the photon statistics and makes the system available for applications, such as the production of conditional states, which is actually feasible as described in the following. Notice that in our system we selected single coherence twin areas in the signal and idler light in order to match the single-mode theoretical description and demonstrated that this experimental condition both minimizes the amount of detected spurious light and maximizes the quantum noise reduction.

The scheme is conceptually simple: the signal and idler beams at the output of the amplifier are individually measured by direct detection. The resulting photon counts m_s and m_i, which are highly correlated, are subtracted from each other to demonstrate quantum noise reduction in the difference $d=m_s-m_i$. We calculate the variance of the difference, σ_d^2, and show that

$$\sigma_d^2 < \langle m_s \rangle + \langle m_i \rangle,$$

where $\langle m_s \rangle$ and $\langle m_i \rangle$ are the average numbers of detected photons in the two output beams. The quantity $\langle m_s \rangle + \langle m_i \rangle$ is the SNL—i.e., the value of σ_d^2 that would be obtained for uncorrelated coherent beams.

II. EXPERIMENTS

The experimental setup is sketched in Fig. 1. A frequency-tripled continuous-wave (cw) mode-locked Nd:YLF laser re-

*Electronic mail: maria.bondani@uninsubria.it

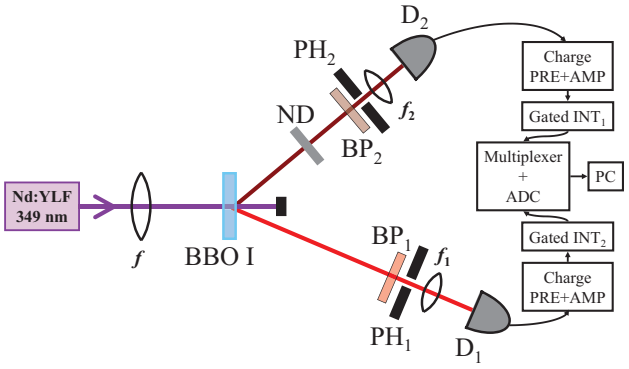

FIG. 1. (Color online) Schematic diagram of the experimental setup. Nd:YLF, frequency-tripled ps-pulsed laser source; BBO I, nonlinear crystal; f, $f_{1,2}$: converging lenses; $PH_{1,2}$, 100-μm-diameter pinholes; $D_{1,2}$, pin detectors; $BP_{1,2}$, bandpass filters; ND, variable neutral-density filter. The boxes on the right side of the figure indicate the parts of the signal amplification and acquisition chains.

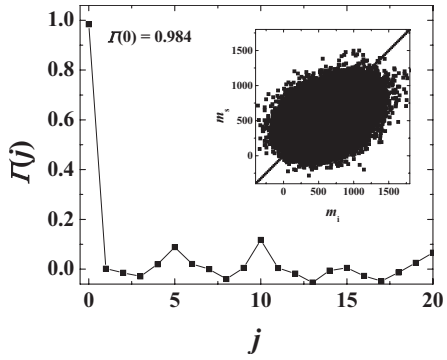

FIG. 2. Correlation function $\Gamma(j)$ as a function of the delay in the laser shots (index j numbers the shots). Inset: values of the photons detected in the signal as a function of those detected in the idler for the same laser shot.

generatively amplified at a repetition rate of 500 Hz (High Q Laser Production, Hohenems, Austria) produces linearly polarized pump pulses at 349 nm with pulse duration of 4.45 ps, as calculated from that of the fundamental pulse [16]. After passing through a $f=250$ mm focal length lens the pump beam comes to a focus (diameter ~ 300 μm) at the position where a 4-mm-thick uncoated β-BaB_2O_4 crystal (BBO I) is placed (Fujian Castech Crystals, Fuzhou, China). The crystal is cut for type I interaction at a 38.4° angle, and it is adjusted to yield efficient parametric amplification of a cw He-Ne laser beam at 632.8 nm that hits the crystal at a 5.85° angle (external angle) to the pump beam. After the BBO I, at distances $d_1=60$ cm and $d_2=49$ cm, respectively, two pinholes of 100 μm diameter are positioned so as to be centered with the amplified signal beam at 632.8 nm and with the idler beam at 778.2 nm. The two different values chosen for the distances compensate the difference in the divergence of signal and idler related to their wavelengths. Stray light is blocked by two suitable bandpass filters BP_1 and BP_2 placed before the pinholes while the light transmitted by the pinholes is conveyed to the detectors D_1 and D_2 by two 25-mm-focal-length lenses that are placed just beyond the pinholes. The interaction seeded by the cw light at the signal wavelength is only used for the preliminary alignment of the pinholes. The D_1 and D_2 detectors are pin photodiodes (S5973-02 and S3883, Hamamatsu Photonics K.K., Japan) with nominal quantum efficiencies of 86% and 90% at the signal and idler wavelengths, respectively. As the combinations of detectors and bandpass filters yield detection efficiencies of 55.0% in the signal arm and of 57.6% in the idler arm, the latter is lowered by adding an adjustable neutral-density filter (ND) in Fig. 1 in order to obtain the same overall detection efficiency $\eta=0.55$ on both arms.

The current outputs of the detectors are amplified by means of low-noise charge-sensitive pre-amplifiers (CR-110, Cremat, Watertown, MA) followed by amplifiers (CR-200-4 μs, Cremat, Watertown, MA), which are identical in the two arms. The two amplified outputs are integrated over gates of 15 μs duration synchronized with the pump pulse by Gated $INT_{1,2}$ in Fig. 1 (SR250, Stanford Research Systems, Palo Alto, CA). The voltage outputs are sampled, digitized, and recorded by a computer. Accurate calibrations of the voltage outputs per electron in the detector current pulses give 33.087 μV/electron for the D_1 arm and 24.803 μV/electron for the D_2 arm. All the data presented in this paper are in units of electrons in the D_1 and D_2 output current pulses, thus corresponding to the number of photons detected in the signal and idler pulses.

The size of the pinholes and their distance from the crystal have been chosen so as to collect twin spatial modes in the down-conversion pattern. In fact, the size of coherence areas in the down-converted light depends on the pump intensity [17,18]. In single-photon experiments this fact usually does not affect the measurement of correlations since the probability of accidental coincidences is very low. On the other hand, when many photons are involved, one should carefully select twin modes—i.e., twin coherence areas. In our measurements, we have optimized the collection of the light by fixing distances and sizes of the pinholes and maximizing correlations against the pump intensity.

III. SUB-SHOT-NOISE CORRELATIONS

The distributions of the detected photons collected by the pinholes are temporally multimode [16]. In order to demonstrate that we selected twin coherence areas we plot in the inset of Fig. 2 the detected photons of the signal (m_s) as a function of those of the idler (m_i) for $K=10^5$ subsequent laser shots. At the pump intensity used in this measurement, the average number of detected photons was $\langle m_s\rangle=528$ and $\langle m_i\rangle=593$. To emphasize the presence of correlations in the parties of the twin beam we evaluated the correlation function

$$\Gamma(j)=\frac{\sum_{k=1}^{K}\{[m_s(k)-\langle m_s\rangle][m_i(k+j)-\langle m_i\rangle]\}/K}{\sqrt{\sigma^2(m_s)\sigma^2(m_i)}}, \qquad (1)$$

where j and k index the shots and $\sigma^2(m)=\langle m^2\rangle-\langle m\rangle^2$ is the variance. Note that Eq. (1) must be corrected by taking into

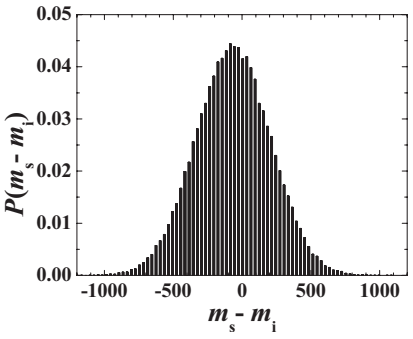

FIG. 3. Distribution of the photon-count difference $P(d)$ measured over 10^5 subsequent laser shots.

account the presence of noise, both in terms of possible correlations and in terms of increased variance. In fact, typical values of the noise rms were $\sigma(m_{\mathrm{s,dark}}) \sim 159$ and $\sigma(m_{\mathrm{i,dark}}) \sim 214$. For the data in the inset, we obtained a value of the correlation coefficient $\Gamma(0)=0.984$, which indicates a high degree of correlation. As we emphasized in [19], a high value of correlation is not sufficient to discriminate between quantum and classical correlations since in both cases $\Gamma(0) \to 1$.

An explicit marker of nonclassicality can be obtained by considering the distribution of the photon-count difference $P(d)$, which is plotted in Fig. 3 for the same data displayed in the inset of Fig 2. The distribution appears symmetrical and centered at zero, which indicates both an accurate balance of the overall efficiencies of the detectors and a high correlation in signal and idler photon numbers. In order to assess the nonclassicality of the twin beam, we calculate the quantum noise reduction R:

$$R = \frac{\sigma_d^2}{\langle m_{\mathrm{s}} \rangle + \langle m_{\mathrm{i}} \rangle}, \tag{2}$$

where, as in the case of the correlation function, the variance of the photon-count difference must be corrected for the electronic noise in the absence of light $\sigma_d^2 \to \sigma_d^2 - \sigma_{d,\mathrm{dark}}^2$.

In principle, we have quantum noise reduction whenever the noise reduction falls in the range $0 < R < 1$ and the whole range is achievable. On the other hand, in order to assess quantitatively the quantum noise reduction, the overall detection efficiency η, which somewhat degrades the observed correlations, should be taken into account. By assuming that both arms of the measurement have the same efficiency and that dark counts have been already subtracted, the probability operator-valued measure (POVM) of each detector is given by a Bernoullian convolution of the ideal number operator spectral measure:

$$\hat{\Pi}_{m_j} = \eta_j^{m_j} \sum_{n_j=m_j}^{\infty} (1-\eta_j)^{n_j-m_j} \binom{n_j}{m_j} |n_j\rangle\langle n_j|, \tag{3}$$

with $j=i,s$. The joint distribution of detected photons $P(m_i,m_s)$ in the idler and signal beams can be evaluated by tracing over the density matrix of the two modes, while the moments of the distribution are evaluated by means of the operators

$$\hat{m_j^p} = \sum_{m_j} m_j^p \hat{\Pi}_{m_j} = \sum_{n_j=0}^{\infty} (1-\eta)^n G_{\eta_j}(n_j) |n_j\rangle\langle n_j|, \tag{4}$$

where

$$G_{\eta}(n) = \sum_{m=0}^{n} \binom{n}{m} \left(\frac{\eta}{1-\eta}\right)^m m^p.$$

Of course, since $\hat{m_j^p}$ are operatorial moments of a POVM, we have, in general, $\hat{m_j^p} \neq \hat{m}_j^p$. The first two moments correspond to the operators

$$\hat{m}_j = \eta_j \hat{n}_j, \tag{5}$$

$$\hat{m_j^2} = \eta_j^2 \hat{n}_j^2 + \eta_j(1-\eta_j)\hat{n}_j. \tag{6}$$

As a consequence, the variances of the two photocurrents are larger than the corresponding photon number variances. We have

$$\sigma^2(m_j) = \eta_j^2 \sigma^2(n_j) + \eta_j(1-\eta_j)\langle \hat{n}_j \rangle.$$

Using this relation we may evaluate the expected noise reduction, which, for our multimode twin beam obtained by spontaneous down-conversion, is given by

$$R = 1 - \eta, \tag{7}$$

independently of the gain of the amplifier.

If $1 > R > (1-\eta)$, the field displays nonclassical correlations [19], whereas $R=1$ marks the boundary between classical and nonclassical behaviors. For the data in Fig. 2, which correspond to maximum noise reduction, we get a value $R=-3.25$ dB below the SNL. Notice that given the overall detection efficiency $\eta=55\%$ $(1-\eta=-3.47$ dB), this is almost the maximum detectable noise reduction and corresponds to an ideal noise reduction (corrected for the quantum efficiency—i.e., measured by 100% efficient detectors at the output of the crystal) equal to $R=-14.4$ dB. Notice also that the use of spontaneous (not seeded) down-conversion allows us to have a quantum noise reduction that is independent of the gain of the parametric amplifier. In fact, for an amplifier seeded by a coherent signal [4,5] the noise reduction is expected to be

$$R = 1 - \eta \left(1 + \frac{1}{2|\nu|^2} \frac{|\alpha|^2}{1+|\alpha|^2}\right)^{-1}, \tag{8}$$

where α is the amplitude of the coherent seed and $|\nu|^2$ is the gain of the OPA. For $\alpha \gg 1$ we have

$$R \simeq 1 - \eta + \eta/(2|\nu|^2)$$

and sub-shot-noise correlations may be observed only for high-gain amplifiers.

The study of R as a function of the pump intensity represents an useful criterion for the selection of a single coherence area. To this aim, in Fig. 4 we show the values of R measured by keeping fixed the collection areas (same pin-

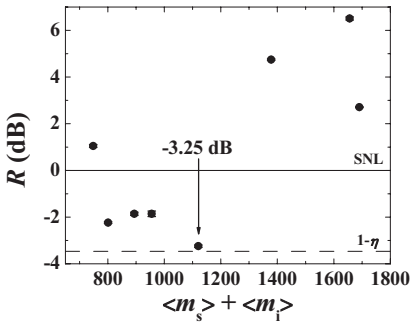

FIG. 4. Quantum noise reduction R (in units of dB) as a function of the average number of detected photons in the signal and idler beams. Solid and dashed lines denote the shot-noise level and the minimum value $R=1-\eta$ of the noise reduction, respectively. Error bars are within the size of the plotted points.

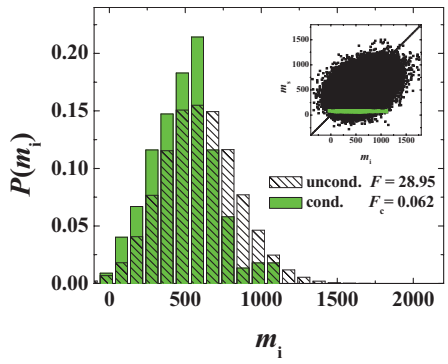

FIG. 5. (Color online) Conditional photon distribution $P(m_\mathrm{i}|m_\mathrm{s}\in\Delta)$ for the idler beam (solid columns), as obtained by selecting detected signal photon in the interval Δ indicated in the inset. We also report the idler unconditional marginal distribution (patterned gray).

holes located at the same distances as for the data in the previous figures) and by varying the intensity of the pumping beam. The figure shows that there is an optimum condition at which R is minimum. In fact, increasing the pump intensity leads to an enlargement of the coherence areas so that they are only partially transmitted by the pinholes (values on the right side of Fig. 4 with respect to the minimum). On the contrary, lowering the pump intensity reduces the size of the coherence areas and hence introduces uncorrelated light in the pinholes (values on the left side of Fig. 4 with respect to the minimum). Note that the values of R corresponding to the selection of more than a single coherence area remain below the SNL or quite close to it as the information contained in the twin areas is not lost, but only made more noisy. On the other hand, selecting only part of the areas causes a loss of information, thus determining an abrupt increase of R above the SNL. We interpret this result as an indication of the need for perfect matching of the pinhole areas in order to obtain sub-shot-noise correlations. Note that, as the detected twin beam is dichromatic, errors in the positioning of the pinholes do not affect the two parties of the twin beam in the same way.

The results reported so far demonstrate the sub-shot-noise—i.e., quantum—nature of the intensity correlations in our twin beam. These features should not be confused with the presence of entanglement, which, though expected in our system, cannot be claimed on the basis of the present measurements (a direct evidence of entanglement would be achievable by measuring two conjugated quadratures by homodyne detection).

IV. CONDITIONAL MEASUREMENTS

The correlated states produced by our system are suitable to generate mesoscopic single-beam nonclassical states by conditional measurements [20,21]. The conditional measurement is made as follows: the number of detected photons in the idler, m_i, is kept only if the number of detected photons in the signal, m_s, falls into a specific interval Δ far from its mean value. The conditional distribution

$$P(m_\mathrm{i}|m_\mathrm{s}\in\Delta)=\sum_{m_\mathrm{s}\in\Delta}P(m_\mathrm{i},m_\mathrm{s})$$

is reported in Fig. 5 together with the unconditional marginal distribution $P(m_\mathrm{i})=\Sigma_{m_\mathrm{s}}P(m_\mathrm{i},m_\mathrm{s})$, $P(m_\mathrm{i},m_\mathrm{s})$ being the joint idler-signal photon distribution. The narrowing of the conditional distribution below the SNL is apparent. The Fano factor $[F=\sigma^2(m)/\langle m\rangle]$ of the idler conditional distribution, suitably corrected for the noise, is given by $F_\mathrm{c}=0.062$ (to be compared to that of the corresponding unconditional marginal distribution $F=28.95$), which corresponds to a noise reduction of about 12 dB below the single-beam shot-noise level. The probability of success—i.e., the fraction of data that are kept to build the distribution—is 0.22%. The success probability may be increased by enlarging the interval of acceptance, at the price of increasing the Fano factor, which goes above unity if the acceptance window is too large or closer to the mean value of the unconditional distribution [20].

Our detection scheme, being based on direct detection of the photons in the two arms of the twin beam, is somehow more noisy as compared to the schemes adopted in [4,5], which make use of electronic subtraction of the pin photocurrents of signal and idler. On the other hand, our technique has the advantage of keeping the information about the marginal probability distributions, whose data can be used for state conditioning and engineering by post-selection of one of the two parties. Of course, when information on the marginal distributions is not required, direct measurement of the difference photocurrent is preferable. Our technique, being based on the ability of properly selecting the twin coherence areas, provides a system suitable for many applications exploiting the sub-shot-noise correlations of the twin beam [22–26]. Indeed, the twin beam may be used as a maximally effective probe to reveal either tiny displacements imposed by light-matter interactions or by external perturbations. For instance, one can implement absorption measurements of weakly absorbing samples by looking at the degradation of the noise reduction or at the variation of the Fano factor in conditional measurements, thus improving the performances

of single-mode techniques [27]. In this framework, the fact that the twin beam is dichromatic, and hence its two parties are tunable in frequency, is undoubtedly relevant.

V. CONCLUSIONS AND OUTLOOKS

In conclusion, we have demonstrated the possibility of obtaining sub-shot-noise intensity correlations in the ps-pulsed mesoscopic regime by properly selecting the twin coherence areas on the parties of the twin beam. Our system, which is based on spontaneous downconversion, does not suffer from limitations due to the finite gain of the parametric process and allows us to demonstrate conditional generation of sub-Poissonian light. The mesoscopic nature of our twin beams makes them a promising system to reveal the presence of small perturbations—e.g., weakly absorbing biological samples—in a nondestructive illumination regime suitable to preserve even photolabile compounds.

ACKNOWLEDGMENTS

This work has been supported by MIUR Project Nos. PRIN-2005024254-002 and FIRB-RBAU014CLC-002.

[1] P. H. Souto Ribeiro, C. Schwob, A. Maître, and C. Fabre, Opt. Lett. **22**, 1893 (1997).
[2] A. Heidmann, R. J. Horowicz, S. Reynaud, E. Giacobino, C. Fabre, and G. Camy, Phys. Rev. Lett. **59**, 2555 (1987).
[3] J. Gao, F. Cui, C. Xue, C. Xie, and P. Kunchi, Opt. Lett. **23**, 870 (1998).
[4] O. Aytür and P. Kumar, Phys. Rev. Lett. **65**, 1551 (1990).
[5] D. T. Smithey, M. Beck, M. Belsley, and M. G. Raymer, Phys. Rev. Lett. **69**, 2650 (1992).
[6] M. Vasilyev, S. K. Choi, P. Kumar, and G. Mauro D'Ariano, Phys. Rev. Lett. **84**, 2354 (2000).
[7] O. Jedrkiewicz, Y. K. Jiang, E. Brambilla, A. Gatti, M. Bache, L. A. Lugiato, and P. Di Trapani, Phys. Rev. Lett. **93**, 243601 (2004).
[8] M. Bondani, A. Allevi, E. Puddu, A. Andreoni, A. Ferraro, and M. G. A. Paris, Opt. Lett. **29**, 180 (2004); **29**, 1417(E) (2004);
[9] A. C. Funk and M. G. Raymer, Phys. Rev. A **65**, 042307 (2002).
[10] A. Porzio, V. D'Auria, P. Aniello, M. G. A. Paris, and S. Solimeno, Opt. Lasers Eng. **45**, 463 (2007).
[11] V. C. Usenko and M. G. A. Paris, Phys. Rev. A **75**, 043812 (2007).
[12] G. M. D'Ariano, M. G. A. Paris, and P. Perinotti, Phys. Rev. A **65**, 062106 (2002).
[13] N. Treps, U. Andersen, B. Buchler, P. K. Lam, A. Maitre, H. A. Bachor, and C. Fabre, Phys. Rev. Lett. **88**, 203601 (2002); A. F. Abouraddy, P. R. Stone, A. V. Sergienko, B. E. A. Saleh, and M. C. Teich, *ibid.* **93**, 213903 (2004).
[14] T. Kim, J. Dunningham, and K. Burnett, Phys. Rev. A **72**, 055801 (2005).
[15] M. Martinelli, N. Treps, S. Ducci, S. Gigan, A. Maitre, and C. Fabre, Phys. Rev. A **67**, 023808 (2003).
[16] F. Paleari, A. Andreoni, G. Zambra, and M. Bondani, Opt. Express **12**, 2816 (2004).
[17] A. Allevi, M. Bondani, A. Ferraro, and M. G. A. Paris, Laser Phys. **16**, 1451 (2006).
[18] A. Joobeur, B. E. A. Saleh, T. S. Larchuk, and M. C. Teich, Phys. Rev. A **53**, 4360 (1996).
[19] A. Agliati, M. Bondani, A. Andreoni, G. De Cillis, and M. G. A. Paris, J. Opt. B: Quantum Semiclassical Opt. **7**, S652 (2005).
[20] J. Laurat, T. Coudreau, N. Treps, A. Maitre, and C. Fabre, Phys. Rev. Lett. **91**, 213601 (2003).
[21] A. Ourjoumtsev, A. Dantan, R. Tualle-Brouri, and P. Grangier, Phys. Rev. Lett. **98**, 030502 (2007).
[22] A. S. Lane, M. D. Reid, and D. F. Walls, Phys. Rev. A **38**, 788 (1988).
[23] P. R. Tapster, S. F. Seward, and J. G. Rarity, Phys. Rev. A **44**, 3266 (1991).
[24] C. D. Nabors and R. M. Shelby, Phys. Rev. A **42**, 556 (1990).
[25] J. J. Snyder, E. Giacobino, C. Fabre, A. Heidmann, and M. Ducloy, J. Opt. Soc. Am. B **7**, 2132 (1990).
[26] A. Porzio, C. Altucci, M. Autiero, A. Chiummo, C. de Lisio, and S. Solimeno, Appl. Phys. B: Lasers Opt. **73**, 763 (2001).
[27] V. D'Auria, C. de Lisio, A. Porzio, S. Solimeno, and M. G. A. Paris, J. Phys. B **39**, 1187 (2006).